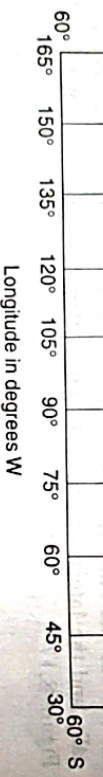


SIDE BAR

The first measurements of raindrop size distributions were made by Laws and Parsons³³ in 1944 with a very ingenious experiment. The experiment was designed to find the sizes of raindrops in typical rainstorms. A baking pan (typically 1 m × 0.5 m) was filled with flour and placed out in the rain for a minute. The pan of flour was then baked in an oven, and the loose flour sifted out. What remained were pellets of baked flour where raindrops had fallen and characteristics.

FIGURE 8.16 Rainfall rate exceedance contours for the Americas (from reference 21 © ITU reproduced with permission). This was the first of a set of three rainfall rate exceedance contours that were developed for the world. In this version, the contours only existed over land. The latest versions²⁰ include data over all of the surface of the earth (see Figure 8.17).



Longitude in degrees W

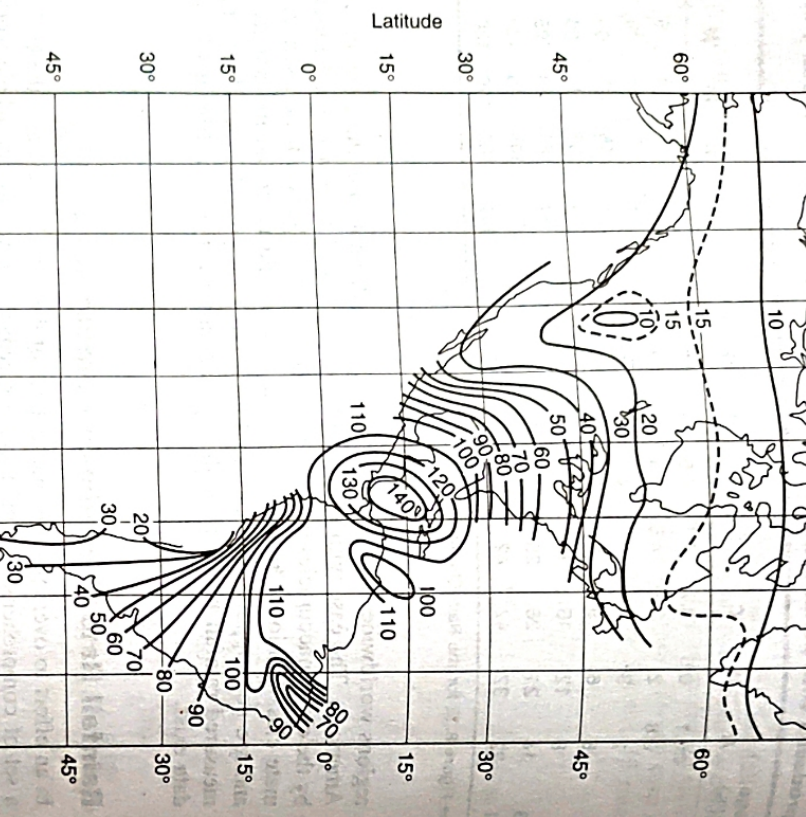


FIGURE 8.17 Rain intensity (mm/h) exceeded for 0.01% of the average year (Figure 2 of reference 22). This map provides rainfall rate contours for the Northern Hemisphere between longitudes 300° E and 80° E (Europe, North Africa, the Middle East, and parts of Russia, India, and China).



Scanned By Scanner Go

8.5 PREDICTION OF RAIN ATTENUATION

Attenuation by rain can be predicted accurately if the rain can be precisely described all the way along the path. Path attenuation is essentially an integral of all the individual increments of rain attenuation caused by the drops encountered along the path. This is the physical approach to predicting rain attenuation. Unfortunately, rain cannot be described accurately along the path without extensive meteorological databases, which do not exist in most regions of the world. Most prediction models therefore resort to semiempirical approaches, which calculate an effective path length through the rain, L_{eff} , over which the rainfall rate is assumed to be constant. This constant rainfall rate leads to a constant specific attenuation, γ_R , and the path attenuation, A , is simply given by

$$\begin{aligned} A &= \text{specific attenuation} \times \text{effective path length in rain} \\ &= \gamma_R L_{\text{eff}} \text{ dB} \end{aligned} \quad (8.12)$$

The semiempirical approach is based on two premises: (1) Rainfall rate measured at a point on the surface of the earth is statistically related (over a period of at least a year) to the attenuation encountered along the path to a satellite from that same point; (2) The actual

length of the path through the rain medium can be adjusted such that an "effective" is developed over which the rain can be considered to be homogeneous (see Figure 8.6).

The estimation of attenuation on the slant path to a satellite is essential to the process of establishing a margin in the link budget that ensures the required availability to the user is met. Over a period of many years, several attenuation models have been developed and have been widely used. These include the Crane model¹⁵, the simple attenuation model (SAM)¹⁶, the Dissanayake, Haidara, Allnutt (DAH) model¹⁷ and several models published by the CCIR and ITU-R^{15,21,23}. The ITU-R model, based on the DAH model¹⁵, is discussed in detail here, because it provides the most accurate statistical estimate of attenuation paths, worldwide, at the time of writing. Appendix D discusses the simple attenuation model (SAM), developed at Virginia Tech by Warren Stutzman and Keith Dismal. The SAM model is less accurate than the ITU-R model, but allows the user to quickly obtain an estimate of the slant-path attenuation at any frequency and rain rate.

A power law equation describes the relationship between point rainfall rate R and specific attenuation, γ_R , the attenuation measured over 1 km²⁴

$$\gamma_R = k(R_{0.01})^\alpha \text{ dB/km} \quad (8.13)$$

In Eq. (8.13), the suffix 0.01 to R denotes the rainfall rate measured for 0.01% of the average year, a typical input time percentage for most models. Equation (8.13) holds for all values of rainfall rate, however. The parameters k and α are frequency dependent. Table 8.3 gives values for k and α for frequencies between 4 and 50 GHz²⁵.

TABLE 8.3 Regression Coefficients for Estimating Specific Attenuation [from TABLE 1 in [25] © ITU, reproduced with permission]

Frequency (GHz)	k_H	k_V	α_H	α_V
4	0.000650	0.000591	1.121	1.075
6	0.00175	0.00155	1.308	1.265
8	0.00454	0.00395	1.327	1.310
10	0.0101	0.00887	1.276	1.264
12	0.0188	0.0168	1.217	1.200
20	0.0751	0.0691	1.099	1.065
30	0.187	0.167	1.021	1.000
40	0.350	0.310	0.939	0.929
50	0.536	0.479	0.873	0.868

NOTES:

- (1) The suffices V and H refer to vertical and horizontal polarization, respectively
- (2) Values of k and α at frequencies other than those in the table can be obtained by interpolation using a logarithmic scale for frequency, a logarithmic scale for k and a linear scale for α .
- (3) Values have been tested and found to be accurate up to a frequency of 40 GHz; values between 40 and 50 GHz are expected to be accurate but have not yet been tested.
- (4) For linear and circular polarization, and for all path geometries, the coefficients in equation (8.13) can be calculated using the values in the above table and the following equations²⁵

$$k = [k_V + k_H + (k_V - k_H)\cos^2\theta \cos 2\tau]/2$$

$$\alpha = [(k_{V,H} + k_{V,H} + (k_{V,H} - k_{V,H})\cos^2\theta \cos 2\tau]/2k$$

where θ is the path elevation angle and τ is the polarization tilt angle relative to the horizontal ($\tau = 45^\circ$ for circular polarization).

EXAMPLE 8.5.1 What is the specific attenuation at 10 GHz if the rainfall rate is 40 mm/h and linear vertical polarization is used?

Answer From Table 8.3, $k_V = 0.00887$ and $\alpha_V = 1.264$ at a frequency of 10 GHz. Using Eq. (8.13), we therefore have

$$\text{Specific attenuation} = \gamma_R = 0.00887(40)^{1.264} = 0.9396 = 0.94 \text{ dB/km}$$

If the rainfall rate were constant along the path, as it generally is in light, stratiform rain (see Figure 8.5), then calculating the total attenuation for a given rainfall rate would be simple. The physical path length through the rain, L , would be the same as the effective path length and the total attenuation, A , is given by

$$A = \gamma_R \times \text{physical path length in rain} = \gamma_R L \text{ dB} \quad (8.14)$$

On short terrestrial paths (<5 km), although this varies with rainfall rate: the lower the rainfall rate, the longer the path), the path length through relatively constant rain can be taken as the distance between the transmitting and receiving antennas. The path through the rain is also at almost the same height along the whole path. This is not the case with satellite paths where the signal follows a slanting path through the atmosphere, and encounters rain of different types and intensities on the way. Rain can take more than 10 min to fall from a height of 5 km (the approximate upper limit of liquid water in a severe thunderstorm) to the ground. If there are updrafts present, as is always the case in convective rain, it can take even longer. There is therefore no instantaneous relationship between attenuation measured along a path to a satellite and the rainfall rate measured at the earth station site. However, there is a strong statistical relationship between the long-term cumulative statistics of rainfall rate and the long-term statistics of slant-path attenuation. Many models of rain attenuation use *equiprobable values* of rainfall rate and path attenuation to determine the cumulative statistics of attenuation from those of rainfall rate. Figure 8.18 illustrates the procedure for finding equiprobable values of rainfall rate and path attenuation.

The assumption that point rainfall rate on the ground is statistically related (over a period of at least a year) to the attenuation observed on a satellite path to that same point has been validated in many experiments worldwide. Since the path encounters highly variable drop sizes and rainfall rates, the physical length L used in Eq. (8.14) has usually to be replaced by an effective path length L_{eff} . We therefore find that the total path attenuation, A , for a given satellite link is given by Eq. (8.12), which is repeated below for completeness

$$A = \gamma_R \times \text{effective path length in rain} = \gamma_R L_{\text{eff}} \text{ dB} \quad (8.15)$$

The procedure by which the effective path length is calculated uses the statistical height of rain (i.e., the melting level height), the height of the earth station above mean sea level, and the elevation angle. See Figure 8.19 and earlier Figures 8.5 and 8.6.

In Figure 8.19, the rain is shown as filling the complete slant path up to the melting layer. This is a correct assumption in stratiform rain, which exists over large areas and has a relatively constant rain rate along the slant path. It is rarely correct when convective rain is present. The rain rate and drop distributions are not constant, and the path may not pass through the top of the rain cell. Figure 8.20 illustrates the problem. The ITU-R procedure for predicting slant-path rain attenuation for GEO satellite paths is contained in Section 2.2.1.1 of Rec. 618¹⁵. It uses a semiempirical approach to the prediction of rain attenuation. Rather than attempt to predict attenuation by inputting rainfall rate at every time percentage, it inputs only the rainfall rate measured (or predicted) for 0.01% of a year. It then extrapolates from this time percentage to other time percentages. While this "one size fits all" approach is nonphysical, it removes the inherent inaccuracies

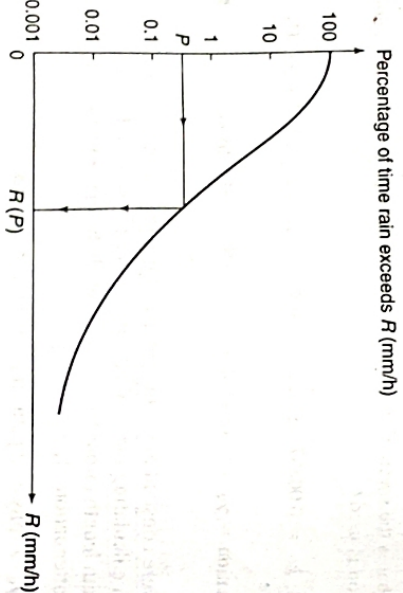


FIGURE 8.18 Cumulative statistics of rainfall rate and path attenuation illustrating equiprobable procedures. For a given time percentage, P , the rainfall rate read off the rainfall rate stat is and the path attenuation stats off the path attenuation is read. If the data for the two parameters have been taken over a long enough period (at least a year; longer periods in multiples of years), $R(P)$ and $A(P)$ are strongly related. Some models use the full rainfall rate statistics to develop path attenuation statistics. Others use one time percentage to relate the two statistics (e.g., the 0.01% point) and develop the second set of statistics from that single point. The disadvantage of this approach (i.e., it is nonphysical) is outweighed by the improved accuracy obtained by extrapolating to both low and high time percentages, where the rainfall rate measurements are somewhat suspect.

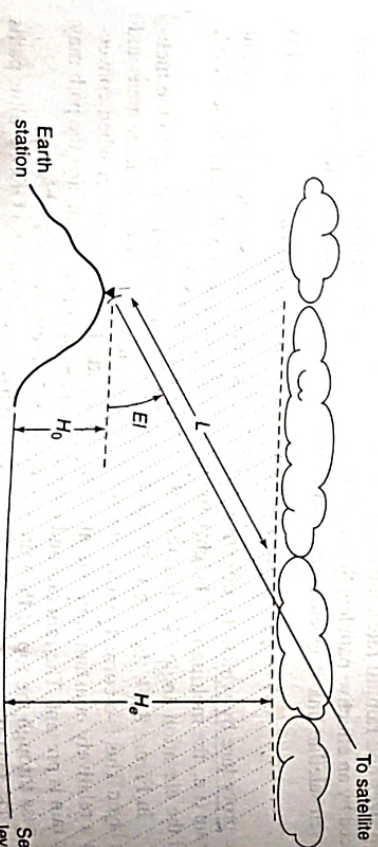


FIGURE 8.19 Geometry of a satellite path through rain. The height of the melting layer, shown as H_R here, is normally considered to be the highest point at which rain attenuation occurs. The rain fills the volume between the melting layer height and the ground. The height of the earth station above mean sea level is given by H_s .

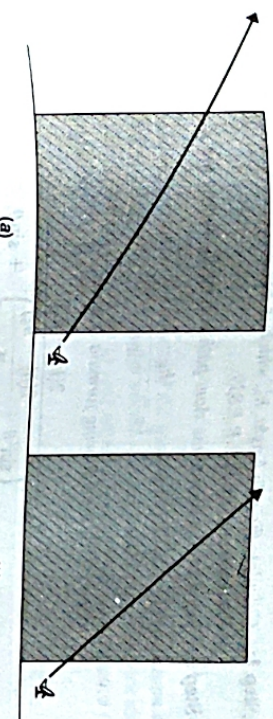


FIGURE 8.20 Example of different path length geometries. In both cases, a similar rainstorm exists in the slant path. In case A, the path to the satellite exits through the side of the storm cell while in case B it exits through the top (in a similar geometry as in Figure 8.5). The only difference between the two paths is the elevation angle to the satellite. To develop an effective path length to use in Eq. (8.12), use is made of both a "vertical adjustment factor" and a "horizontal adjustment factor" to account for the possibility of either case A or case B occurring.

of using very low rainfall rates for time percentages of 0.1% (and higher) or very high rainfall rates for time percentages of 0.001%. The ITU-R is seeking to change this one size fits all approach. The current procedure (early 2002) is reproduced below (the equation and figure numbers have been changed to correspond with those in this chapter).

The following procedure provides estimates of the long-term statistics of the slant-path rain attenuation at a given location for frequencies up to 55 GHz. The following parameters are required:

$R_{0.01}$: point rainfall rate for the location for 0.01% of an average year (mm/h)
 h_s : height above mean sea level of the earth station (km)
 θ : elevation angle (degrees)
 ϕ : latitude of the earth station (degrees)
 f : frequency (GHz).
 R_c : effective radius of the earth (8500 km)

The geometry is illustrated in Figure 8.21.

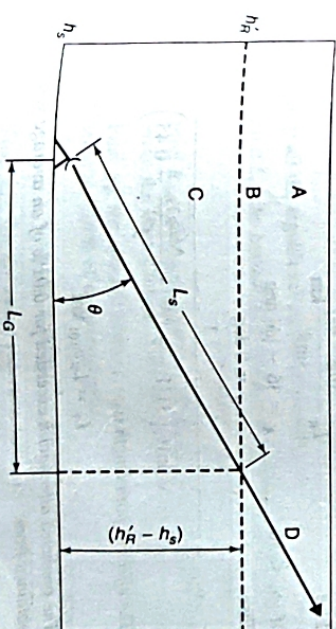


FIGURE 8.21 Schematic presentation of an earth-space path giving the parameters to be input into the ITU-R rain attenuation prediction procedure (Figure 1 of reference 15 © ITU, reproduced with permission).

Step 1: Calculate the rain height, h'_k , which is equivalent to h_0 as given in Recommendation ITU-R P.839.

Step 2: For $\theta \geq 5^\circ$ compute the slant-path length, L_S , below the rain height from:

$$L_S = \frac{(h'_k - h_s)}{\sin \theta} \text{ km} \quad (8.16)$$

For $\theta < 5^\circ$, the following formula is used:

$$L_S = \frac{2(h'_k - h_s)}{\left(\sin^2 \theta + \frac{2(h'_k - h_s)}{R_e}\right)^{1/2}} \text{ km} \quad (8.17)$$

Step 3: Calculate the horizontal projection, L_G , of the slant-path length from:

$$L_G = L_S \cos \theta \text{ km} \quad (8.18)$$

Step 4: Obtain the rainfall rate, $R_{0.01}$ exceeded for 0.01% of an average year (with an integration time of 1 min). If this long-term statistic cannot be obtained from local data sources, an estimate can be obtained from the maps of rainfall rate given in Recommendation ITU-R P.837.

Step 5: Obtain the specific attenuation, γ_k , using the frequency-dependent coefficients given in Recommendation ITU-R P.838 and the rainfall rate, $R_{0.01}$, determined from Step 4, by using:

$$\gamma_k = k(R_{0.01})^a \text{ dB/km} \quad (8.19)$$

Step 6: Calculate the horizontal reduction factor, $r_{0.01}$, for 0.01% of the time:

$$r_{0.01} = \frac{1}{1 + 0.78\sqrt{\frac{L_G \gamma_k}{f}} - 0.38(1 - e^{-2\zeta})} \quad (8.20)$$

Step 7: Calculate the vertical adjustment factor, $v_{0.01}$, for 0.01% of the time:

$$\zeta = \tan^{-1} \left(\frac{h'_k - h_s}{L_G r_{0.01}} \right) \text{ deg}$$

For $\zeta > 0$

$$L_R = \frac{L_G r_{0.01}}{\cos \theta} \text{ km}$$

Else

$$L_R = \frac{(h'_k - h_s)}{\sin \theta} \text{ km}$$

If $|\phi| < 36^\circ$

$$\chi = 36 - |\phi| \text{ deg}$$

Else

$$\chi = 0 \text{ deg}$$

$$v_{0.01} = \frac{1}{1 + \sqrt{\sin(\theta)} \left(31(1 - e^{-(0.01 + \chi)}) \frac{\sqrt{L_R \gamma_k}}{f^2} - 0.45 \right)} \quad (8.21)$$

Step 8: The effective path length is

$$L_E = L_R v_{0.01} \text{ km} \quad (8.21)$$

Step 9: The predicted attenuation exceeded for 0.01% of an average year is obtained from:

$$A_{0.01} = \gamma_k L_E \text{ dB} \quad (8.22)$$

Step 10: The estimated attenuation to be exceeded for other percentages of an average year, in the range 0.001% to 5%, is determined from the attenuation to be exceeded for 0.01% for an average year.

If $p \geq 1\%$ or $|\phi| \geq 36^\circ$:

$$\beta = 0$$

If $p < 1\%$ and $|\phi| < 36^\circ$ and $\theta \geq 25^\circ$:

$$\beta = -0.005(|\phi| - 36)$$

Otherwise:

$$\beta = -0.005(|\phi| - 36) + 1.8 - 4.25 \sin(\theta) \quad (8.23)$$

This method provides an estimate of the long-term statistics of attenuation due to rain. When comparing measured statistics with the prediction, allowance should be given for the rather large year-to-year variability in rainfall rate statistics (see Recommendation ITU-R P.678).

EXAMPLE 8.5.2

A Ku-band satellite is to be used in a video broadcasting system. The uplink will be from Miami, Florida, where the studios of the company are located. Since the uplink will be used to feed more than a million home receivers, the uplink availability must be 99.99% in the average year. The question is therefore: what is the rain attenuation on the Miami uplink path for 0.01% of the average year? The information on the link is as follows:

Uplink frequency	17.80 GHz
Polarization	Vertical
Coefficients for calculating specific attenuation at 17.80 GHz	$k_v = 0.0510$
Rain climate regions for Miami	$\alpha_v = 1.0927$
Elevation angle	45°
Height of rain h'_k	Assume 4 km in Miami
Height of Miami earth station site a.m.s.l.	0.05 km
(above mean sea level)	

Answer

Step 1: We already know the rain height (given as 4 km).

Step 2: Find L_S , the slant-path length below the rain height.

$$L_S = \frac{(h'_k - h_s)}{\sin \theta}, \text{ thus } L_S = 5.5861 \text{ km}$$

(Note: Keep all the significant figures at present.)

Step 3: Find L_G , the horizontal projection of the slant-path length.

$$L_G = L_S \cos \theta, \text{ thus } L_G = 3.95 \text{ km}$$

Step 4: Find $R_{0.01}$, the rainfall rate for 0.01% of an average year (mm/h).

From the Rain Climatic Zone information (Table 8.2), we have $R_{0.01} = 63 \text{ mm/h}$.

Step 5: Find γ_k , the specific attenuation, along the path for Miami for the rainfall rate encountered at 0.01% of an average year.

Step 6: Find $r_{0.01}$, the horizontal reduction factor for Miami.

$$r_{0.01} = \frac{1}{1 + 0.78\sqrt{\frac{L_G \gamma_k}{f}} - 0.38(1 - e^{-2\zeta})}$$

Thus $r_{0.01} = 0.7051$ for Miami.

Step 7: Calculate the vertical adjustment factor, $v_{0.01}$, for Miami.

To do this we need some intermediate parameters.

Part (a): Calculate ζ , where

$$\zeta = \tan^{-1} \left(\frac{h'_k - h_k}{L_k r_{001}} \right)$$

Thus, $\zeta = 54.81230$ for Miami. This is greater than the elevation angle, θ , which is 45° .

Part (b): Find L_k , an intermediate parameter in calculating the effective path length.

Since $\zeta > \theta$,

$$L_k = \frac{L_k r_{001}}{\cos \theta}$$

giving $L_k = 3.9388$ km.

Part (c): Find χ , the second intermediate parameter for calculating effective path length.

$$\chi = 36 - |\phi|$$

where ϕ is the latitude of the site. Thus $\chi = 36 - 25 = 11.0$ for Miami.

Finally, calculate v_{001} , from

$$v_{001} = \frac{1}{1 + \sqrt{\sin(\theta)} \left(31 \left(1 - e^{-(\theta)(1+x)} \right) \frac{\sqrt{L_k} Y_R}{f^2} - 0.45 \right)}$$

This gives $v_{001} = 1.0332$ for Miami.

Step 8: Calculate L_E , the effective path length for Miami.

$$L_E = L_k v_{001}$$

which gives $L_E = 4.0696$ for Miami.

Step 9: Calculate A_{001} , the predicted attenuation exceeded for 0.01% of an average year along the path in Miami.

$$A_{001} = \gamma_R L_E$$

and this gives

$$A_{001} = 19.1983 \text{ dB for Miami} \Rightarrow 19.2 \text{ dB}$$

The rain attenuation on the uplink from Miami for 0.01% of the average year will be 19.2 dB, which is the answer to the question posed. This value, however, pertains to a fixed link that does not change significantly with time. Such a situation would not apply to non geostationary orbit (NGSO) satellite systems. A double-probabilistic approach is required for estimating the statistical impact of rain attenuation on NGSO paths: the probability that attenuation will occur for a given elevation angle and the probability that the satellite will be at that elevation angle. The first approach is documented in ITU-R Rec. 618¹⁵ and is abstracted below.

Calculation of Long-Term Statistics for NGSO Systems

For non-NGSO systems, where the elevation angle is varying, the link availability for a single satellite can be calculated in the following way:

- calculate the minimum and maximum elevation angles at which the system will be expected to operate;
- divide the operational range of angles into small increments (e.g., 5° wide);
- calculate the percentage of time that the satellite is visible as a function of elevation angle in each increment;

- for a given propagation impairment level, find the time percentage that the level is exceeded for each elevation angle increment;
- for each elevation angle increment, multiply the results of c) and d) and divide by 100, giving the time percentage that the impairment level is exceeded at this elevation angle;
- sum the time percentage values obtained in e) to arrive at the total system time percentage that the impairment level is exceeded.

In the case of multi-visibility satellite constellations employing satellite path diversity (i.e., switching to the least impaired path), an approximate calculation can be made assuming that the spacecraft with the highest elevation angle is being used.

Scaling Attenuation with Elevation Angle and Frequency

Experience has shown that, if long-term attenuation data already exist at a site, it is more accurate to scale measured results to another frequency or another elevation angle, instead of predicting the path attenuation at the new frequency and/or elevation angle from rainfall rate data. Two fairly simple (and surprisingly accurate) rules of thumb exist for scaling over small changes in frequency and elevation angle:

- For a uniform rainfall rate environment (i.e., stratiform rain) and assuming a "flat earth," path attenuation in decibels scales with the path length through the rain (i.e., it follows a cosecant law);
- Between about 10 and 50 GHz, attenuation in decibels scales as the square of the frequency. These two laws are expanded below.

Cosecant Law

The attenuation in decibels at the same frequency at elevation angles E_1 and E_2 from the same site are approximately related by

$$\frac{A(E_1)}{A(E_2)} = \frac{\csc(E_1)}{\csc(E_2)} \quad (8.24)$$

This formula breaks down when the elevation angle is low ($< 10^\circ$) where its implicit flat earth and uniform rainfall rate assumptions fail to hold.

EXAMPLE 8.5.3

A 12-GHz direct broadcast satellite link was found to experience 4 dB of rain attenuation at an elevation angle of 45° for 0.01% of the time in an average year. What would be the rain attenuation measured at the same time percentage for the same site if the elevation angle were 10° ?

Answer Let suffix 1 in Eq. (8.24) refer to the new elevation angle (i.e., 10°) and suffix 2 to the old elevation angle. Thus,

$$\begin{aligned} A(10^\circ) &= [\csc(10^\circ)/\csc(45^\circ)] \times A(45^\circ) \\ &= [5.7583/1.4142] \times 4 \text{ dB} \\ &= 16.2883 \Rightarrow 16.3 \text{ dB} \end{aligned}$$

The impact of elevation angle on a given link is clear from this example.

Squared Frequency Scaling Law

If $A(f_1)$ and $A(f_2)$ are the attenuations that would be measured on the same path at frequencies f_1 and f_2 GHz, they are approximately related by

$$\frac{A(f_1)}{A(f_2)} = \frac{(f_1)^2}{(f_2)^2}. \quad (8.25)$$

This formula relates the *long-term* statistics (i.e., annual statistics). It should not be used for short-term frequency scaling (i.e., from second to second) on a link or for frequencies that are close to any resonant absorption line.

EXAMPLE 8.5.4

A user measures rain attenuation statistics along a satellite link as 6 dB for 0.01% of a year when using a carrier frequency of 10.7 GHz. The satellite operator wants to move the user from the current transponder to a new one, which would change the carrier frequency to 11.4 GHz. What would be the new rain attenuation value, all other link parameters remaining the same?

Answer Let suffix 1 in Eq. (8.25) refer to the new frequency (i.e., 11.4 GHz) and suffix 2 refer to the old frequency (i.e., 10.7 GHz). Thus,

$$\begin{aligned} A(11.4) &= [(11.4)^2 / (10.7)^2] \times A(10.7) \\ &= [129.9600 / 114.4900] \times 6 \text{ dB} \\ &= 6.807 \Rightarrow 6.8 \text{ dB} \end{aligned}$$

ITU-R Long-Term Frequency Scaling of Rain Attenuation

If A_1 and A_2 are the equiprobable values of rain attenuation, in dB, at frequencies f_1 and f_2 (GHz), respectively, the attenuation at frequency f_2 can be found from that at frequency f_1 from

$$A_2 = A_1(\phi_2/\phi_1)^{1-H(\phi_2, \phi_1, A_1)} \quad (8.26)$$

where

$$\phi(f) = \frac{f^2}{1 + 10^{-f^2}} \quad (8.27)$$

$$H(\phi_1, \phi_2, A_1) = 1.12 \times 10^{-3} (\phi_2/\phi_1)^{0.5} (\phi_1 A_1)^{0.55} \quad (8.28)$$

8.6 PREDICTION OF XPD

Any particle that has spherical symmetry will cause no depolarization of an incident signal. Rain in the atmosphere starts as very small droplets. The surface tension within these droplets is so strong that they retain their spherical shapes. As the drops collide, they coalesce into larger drops. The larger the drop, the more likely it is to distort out of a spherical shape due to wind effects. In convective events, particularly severe thunderstorms,雨滴 can become relatively large (many millimeters in average diameter) and so they will distort into ellipsoidal forms, generally flattening out in the horizontal axis. Figure 8.22 illustrates the process.

Very small droplet: wind effects cannot overcome surface tension and droplet remains perfectly spherical in shape.

Many droplets have collided and coalesced into larger drop. As drop falls, pressure on underside overcomes surface tension forces and drop begins to distort from spherical shape, taking on elliptical profile in vertical axis. Viewed from below, drop is still essentially circular in cross-section.



FIGURE 8.22 Schematic of the shape of an individual raindrop from formation to maturity.

Large, oscillating drops will distort into shapes with no true axes of symmetry. Drops will hollow out underneath due to drop's fall and since such large raindrops generally form as result of severe convective activity, turbulent air motion will cause large, oscillating drops to break up. Smaller drops resulting from this breakup then cause additional raindrop formation to occur.

If all of the ellipsoidal drops in a rainstorm were aligned, then waves propagating with their electrical field vectors parallel to the raindrops' minor axes (for all practical purposes, vertically polarized waves) would experience the minimum attenuation for that rainfall rate, and waves propagating with their electric field vectors parallel to the major axes (i.e., horizontally polarized waves) would experience the maximum attenuation. In these two special cases, no depolarization would occur. The difference between the attenuations experienced by waves with horizontal and vertical polarization is small—rarely greater than a decibel. It is called the differential attenuation. In a like manner, waves with horizontal and vertical polarization can experience differential phase shift as they pass through an anisotropic medium. At frequencies below about 10 GHz, differential phase shift is the more important phenomenon. At frequencies above about 30 GHz, differential attenuation is more important. Between 10 and 30 GHz, either differential phase or differential attenuation will be the major effect, depending on the elevation angle of the link and the climate.³¹

Imagine now the case of a wave whose linear polarization is intermediate between horizontal and vertical. We can resolve this wave into its vertically polarized and horizontally polarized components as in Figure 8.23. These components propagate through the rain with their polarizations unchanged, but the horizontal component is attenuated more than the vertical component. If at any point we recombine the vertical and horizontal components to reconstruct the wave, we find that its polarization has rotated toward the vertical and a cross-polarized component is now present. This process is a simplification of a complicated problem in electromagnetic wave scattering. For details of the process, the reader should consult the extensive publications of T. Oguchi, the pioneer researcher in the field (e.g., [26]).

Depolarization, while it is dependent to a great extent on the volume of rain that is present in the path, the shape of the raindrops in the path and the orientation of their major and minor axes also significantly affect it. The orientation will have two independent features: one that is due to the rain medium, and is referred to as the *tilt angle*, and one that is due to the path geometry, and is referred to as the *tilt angle*.

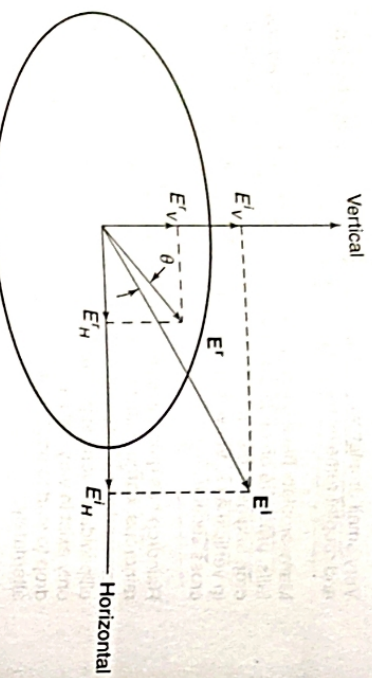


FIGURE 8.23 A simplified explanation of rain depolarization based on a drop with an elliptical cross section. An incident electromagnetic wave with electric field vector E^i strikes a raindrop. We resolve it into a horizontal component E'_H and a vertical component E'_V . The horizontal component is attenuated more than the vertical component because it encounters more water. Thus, when we recombine the horizontal and vertical field components E'_H and E'_V that arrive at the receiver, we find that the received wave E' has had its polarization rotated toward the vertical by the angle θ .

Canting Angle

Falling raindrops orient themselves so as to minimize the aerodynamic forces. In steady fall, the minor axis of the drop is parallel to the net wind force and so their major axis is horizontal when the raindrop is falling in still air. Under windy conditions, the aerodynamic force will have two components: one due to the raindrop fall velocity (i.e., vertical) and one due to the prevailing wind direction (i.e., horizontal). The resultant of these two forces will lead to the raindrops' major axis being canted out of the usual horizontal orientation. The prevailing wind lessens with altitude, becoming zero at the ground. The raindrop orientation will therefore vary with altitude. Since the horizontal wind direction with respect to the path varies, the net horizontal component measured over a long interval will be close to zero. The canting angle will therefore have a mean of zero. In any given rainstorm, however, the canting angle will have a finite probability of being nonzero, thus leading to enhanced depolarization for horizontal or vertical polarized waves over short time intervals. Figure 8.24 illustrates the canting angle process schematically.

Tilt Angle

The tilt angle refers to the angle between the local horizontal (or vertical) and the actual orientation of the electric field vector of the transmitted signal. The orientation of the electric field vector transmitted by a geostationary satellite is referenced to the equator at the subsatellite point. Horizontal polarization is parallel to the equator and vertical polarization is perpendicular to the equator. An earth station that lies on the same longitude as the GEO satellite (say, to the north) would receive signals polarized in the local vertical direction if the satellite is transmitting a vertically polarized signal. If the location of the earth station is moved either east or west from the longitude of the GEO satellite, the vertically polarized signal transmitted by the satellite is now received out of the vertical at the earth station. That is, the polarization vector would appear to be tilted away from the original orientation. The process is illustrated in Figure 8.25.

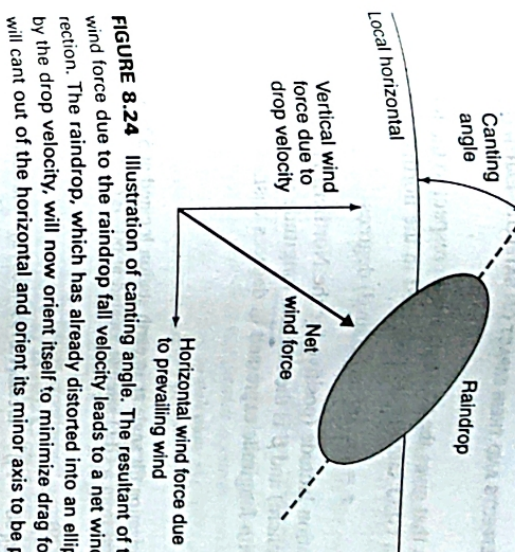


FIGURE 8.24 Illustration of canting angle. The resultant of the prevailing wind force and the wind force due to the raindrop fall velocity leads to a net wind force that is out of the vertical direction. The raindrop, which has already distorted into an ellipsoid due to the wind force induced by the drop velocity, will now orient itself to minimize drag forces. This means that the raindrop will cant out of the horizontal and orient its minor axis to be parallel to the net wind force.

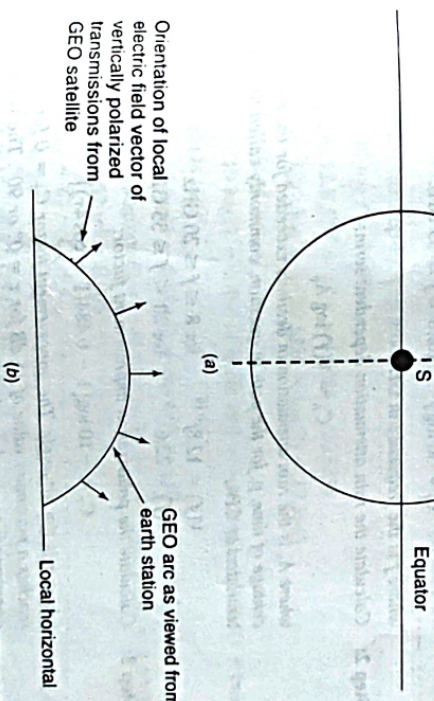


FIGURE 8.25 Schematic of tilt angle. In (a) above, S is the subsatellite point of a GEO satellite. Transmissions from the satellite will be horizontally polarized if they are parallel to the equatorial plane. Vertically polarized transmissions will be orthogonal to the equatorial plane. If an earth station were on the satellite longitude (here shown by the broken line SM) it would receive the polarization vector in the orientation transmitted—although the polarization would be undefined at the subsatellite point. In (b) above, the earth station is not on the equator. The arc shows how the GEO orbit would look from the earth station. In this instance, the satellite is transmitting a vertically polarized signal. The orientation of the vertically polarized transmissions may not be received at the local vertical, however. The local orientation will depend on where the satellite is located on the GEO arc as seen by the earth station. The polarization vector may therefore be tilted out of the transmitted orientation by virtue of the link geometry. The polarization will only be vertical (or horizontal) at the earth station site to a GEO satellite if the azimuth to the satellite is 0° or 180° from true north.

A simple equation that gives the tilt angle τ with respect to the horizontal, assuming the transmissions from a GEO satellite are polarized in the north-south direction, is²⁷

$$\tau = \arctan(\tan L_e / \sin \beta) \text{ degrees} \quad (8.29)$$

where L_e is the earth station latitude (positive for the Northern Hemisphere and negative for the Southern Hemisphere) and β is the satellite longitude minus the earth station longitude (i.e., $L_s - L_e$), with longitude expressed in degrees east.

EXAMPLE 8.6.1

What is the perceived polarization tilt angle at an earth station located at 52° N, 1° E, for vertically polarized signals transmitted from a GEO satellite located at 60° E?

Answer: Using Eq. (8.29)

$$\tau = \arctan(\tan 52 / \sin[60 - 1]) = \arctan(1.2799 / 0.8572) = \arctan(1.4932) = 56.19^\circ$$

The ITU-R XPD prediction method¹⁵ is based on the attenuation measured (or predicted) at the frequency of interest, plus additional terms to take account of the canting angle distribution, the tilt angle, and ice crystal depolarization²⁸. The step-by-step procedure is summarized below.

Step 1: Calculate the frequency-dependent term:

$$C_f = 30 \log f \quad \text{for } 8 \leq f \leq 35 \text{ GHz} \quad (8.30)$$

where f is the frequency in GHz.

Step 2: Calculate the rain attenuation dependent term:

$$C_\alpha = V(f) \log A_p \quad (8.31a)$$

where A_p is the rain attenuation in decibels exceeded for the required percentage of time, p , for the path in question, commonly called the copolar attenuation or CPA;

$$V(f) = 12.8f^{0.19} \quad \text{for } 8 \leq f \leq 20 \text{ GHz} \quad (8.31b)$$

$$V(f) = 22.6 \quad \text{for } 20 < f \leq 35 \text{ GHz} \quad (8.31c)$$

Step 3: Calculate the polarization improvement factor:

$$C_r = -10 \log[1 - 0.484(1 + \cos 4\tau)] \quad (8.32)$$

where τ is the tilt angle. The improvement factor $C_r = 0$ for $\tau = 45^\circ$ and reaches a maximum value of 15 dB for $\tau = 0^\circ$ or 90° . The value $\tau = 45^\circ$ corresponds to circular polarization.

Step 4: Calculate the canting angle dependent term:

$$C_\theta = -40 \log(\cos \theta) \quad \text{for } \theta \leq 60^\circ \quad (8.33)$$

where θ is the elevation angle of the link.

Step 5: Calculate the canting angle dependent term:

$$C_\sigma = 0.0052 \sigma^2 \quad (8.34)$$

where σ is the effective standard deviation of the raindrop canting angle distribution, expressed in degrees. The value of σ is 0°, 5°, 10°, and 15° for 1, 0.1, 0.01, and 0.001% of the time, respectively.

Step 6: Calculate rain XPD not exceeded for $p\%$ of the time:

$$XPD_{\text{rain}} = C_f - C_\alpha + C_r + C_\theta + C_\sigma \text{ dB}$$

- Step 7:** Calculate the ice crystal dependent term:

$$C_{ice} = XPD_{\text{rain}} \times (0.3 + 0.1 \log p)/2 \text{ dB} \quad (8.36)$$

- Step 8:** Calculate the XPD not exceed for $p\%$ of the time, including the effects of ice crystals:

$$XPD_p = XPD_{\text{rain}} - C_{ice} \text{ dB} \quad (8.37)$$

The rain attenuation below 8 GHz is fairly low and so the attenuation-dependent XPD prediction method does not provide accurate results. To calculate XPD for frequencies below 8 GHz, it is best to calculate the XPD at 8 GHz and then scale in frequency to the required frequency using²⁹

$$XPD_2 = XPD_8 - 20 \log \left[\frac{f_2 \sqrt{1 - 0.484(1 + \cos 4\tau)}}{\int_8 f_1 \sqrt{1 - 0.484(1 + \cos 4\tau)} \, df} \right] \quad \text{for } 4 \leq f_1, f_2 \leq 30 \text{ GHz} \quad (8.38)$$

(Unpublished results from the Italstat experiment³⁰ appear to show that it is possible to predict XPD from 35 GHz up to 50 GHz by amending Eq. (8.33) and changing the values of $V(f)$ in Eq. (8.31a) to

$$C_f = 25 \log f \quad (8.39a)$$

$$V(f) = 20 \quad (8.39b)$$

- What is the value of XPD at 0.01% of the time for a 1.2-GHz link that experiences 7-dB attenuation for this period of time? The elevation angle is 30°. Calculate the XPD for tilt angles of 20° and 0°.

- Answer** Using the step-by-step procedure we have:

$$C_f = 30 \log f = 32.3754$$

$$C_\alpha = V(f) \log A_p = 20.5236 \times \log(7) = 17.3445$$

$$C_r = -10 \log[1 - 0.484(1 + \cos 4\tau)] = -10 \log[1 - 0.484(1 + \cos 80)] = 3.6456$$

$$C_\theta = -40 \log(\cos 30) = -40 \log(\cos 30) = -40 \log(0.8660) = 2.4988$$

$$C_\sigma = 0.0052 \sigma^2 = 0.0052 \cdot 0^2 = 0.52$$

$$XPD_{\text{rain}} = C_f - C_\alpha + C_r + C_\theta + C_\sigma$$

$$\text{For } \tau = 20^\circ = 32.3754 - 17.3445 + 14.9485 + 2.4988 + 0.52 = 21.6953 = 21.7 \text{ dB}$$

$$\text{For } \tau = 0^\circ = 32.3754 - 17.3445 + 14.9485 + 2.4988 + 0.52 = 32.9982 = 33.0 \text{ dB}$$

$$\text{Step 7: } C_{ice} = XPD_{\text{rain}} \times (0.3 + 0.1 \log p)/2$$

$$\text{For } \tau = 20^\circ = 21.6953 \times (0.3 + 0.1 \log p)/2 = 21.6953 \times (0.3 + 0.1 \log 0.01)/2$$

$$= 21.6953 \times (0.3 - 0.2)/2 = 1.0848$$

$$\text{For } \tau = 0^\circ = 32.9982 \times (0.3 + 0.1 \log p)/2 = 32.9982 \times (0.3 + 0.1 \log 0.01)/2$$

$$= 32.9982 \times (0.3 - 0.2)/2 = 1.6499$$

Note: The single, best way to reduce depolarization is to operate with polarization sensors that are linear vertical or horizontal as perceived by the receiving antenna. This can be seen from the very different results calculated in the above example when the tilt angle was 0° (i.e., the signal is being received in linear, horizontal polarization) compared with those when the tilt angle is 20°.

Ice Crystal Depolarization

The calculation procedure for ice crystal depolarization incorporated in the calculation XPD has been found to have wide variations in accuracy. At high elevation angles and frequencies below 10 GHz, the procedure tends to agree with measured data. That is, ice crystal depolarization occurs only in severe thunderstorms and so it is a rare occurrence. However, on low elevation angle paths, the contribution due to ice crystals has been observed to occur for quite high time percentages. At frequencies above 30 GHz, it is expected that ice crystal depolarization will be a significant effect, particularly at elevation angles below 30°.

Rain Effects on Antenna Noise

At frequencies below about 50 GHz, rain attenuation is mostly caused by absorption rather than by scattering of the signal energy out of the path. Any absorber with a physical temperature greater than absolute zero (0 kelvins) will act as a black body radiator. At frequencies below 300 GHz, the radiation is in the form of white Gaussian noise with a noise power given by kTB , where T is the equivalent noise temperature of the absorber. Raindrops are absorbers at microwave frequencies and, when the raindrops fall through the antenna beam, some of their isotropically radiated thermal energy will be detected by the receiver (see Chapter 4). Rain will therefore cause not only signal attenuation and depolarization; it will also cause an increase in sky temperature, which, in turn, will increase the overall system noise temperature. The impact of the increase in sky noise temperature can be high for low noise receiving systems at Ku band, as illustrated in the example.

EXAMPLE 8.6.3

What is the additional noise temperature contribution of an antenna compared with that in clear sky when there is 4 dB of rain attenuation in the path? You may assume that the rain medium is at a temperature equivalent to 285 K.

Answer An attenuation of 4 dB causes the signal to be reduced by a factor of 2.5119. The fractional transmission coefficient, σ , would therefore be $1/2.5119 = 0.3981$. (Another way of looking at this is to say that only 39.81% of the original signal power is being received during the 4-dB rain event.) The additional sky temperature radiated would therefore be $285(1 - 0.3981) = 171.5395$ K = 171.5 K. Note that, if the system noise temperature had been 200 K, the effective system noise temperature is now $200 + 171.5 = 371.5$ K. In other words, the signal power has decreased by 4 dB and the noise power has increased by 2.7 dB. A 4-dB rain attenuation has thus led to a 6.7 dB reduction in C/N. This is somewhat simplistic, since the receiving antenna efficiency is not 100%, and it therefore does not accept all of the radiation that is incident upon it. However, the enhanced sky noise contribution received by the antenna during rain conditions will be close to that radiated by the rainstorm. Careful attention must be paid in the system design to allow for enhanced sky noise contributions as well as signal degradations when developing link budgets. Put another way, the key in link budget calculations is to find the change in carrier-to-noise, C/N, rather than just the change in carrier power, C.

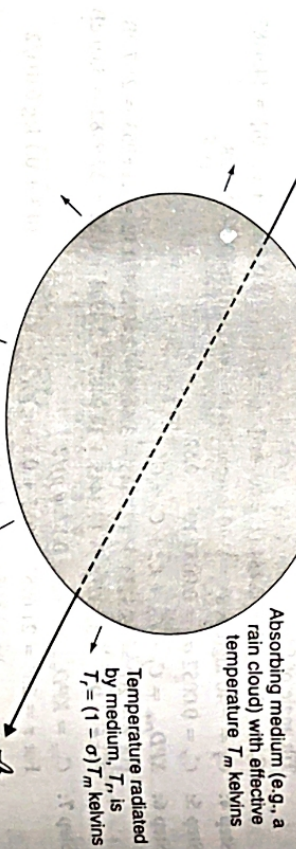


FIGURE 8.26 Schematic of the additional radiated sky temperature due to absorption in rain. The added temperature received by the antenna due to radiation from the "hot" rain storm will cause an additional component to be added to the system noise temperature. This additional component is similar to the noise temperature contribution from a lossy feed, in Chapter 4, in the analysis of system noise temperature, a noise temperature contribution due to signal loss, T_s , was calculated using a "gain" component G , where G was a linear value. For example, when the component at a physical temperature of 280 K caused a loss of 2 dB (which = $1/1.58 = 0.63$ of the original value), $T_s = T_p(1 - G) = 280(1 - 0.63) = 103.6$ K. The parameter G is identical to σ , i.e. a loss of 2 dB is the same as a fractional transmission of 0.63 of the original signal.

Chapter 4. Rain attenuation in the 1 to 3 dB range can cause the system noise level to increase by 1 to 3 dB, leading to a reduction in C/N ratio (in dB) in rain, which is twice the rain attenuation value.

The increase in antenna noise temperature due to rain, T_b , may be estimated by

$$T_b = 280(1 - e^{-A/4.34}) \text{ K} \quad (8.40)$$

where A is the rain attenuation in decibels and the value 280 K is an effective temperature of the rain medium in kelvins. Values between 273 and 290 K may be used, depending on whether the climate is cold or tropical.

An alternative approach is to treat the rain as a passive attenuator with a fractional transmission coefficient of σ . If the rain totally attenuates the signal, $\sigma = 0$; if the rain medium is completely transparent and no attenuation takes place, $\sigma = 1$. Figure 8.26 illustrates the process.

8.7 PROPAGATION IMPAIRMENT COUNTERMEASURES

Attenuation

Many research groups have investigated the use of fade countermeasures. Fade mitigation has been shown³⁰ to fall into three main classes:

- Power control (i.e., varying the EIRP of the signal to enhance C/N)
- Signal processing (i.e., changing the parameters of a signal to improve BER)
- Diversity (i.e., choosing a different path or time to take advantage of decorrelated fading)

Interestingly, the three main classes of fade mitigation affect a link differently and are complementary in nature.³⁰ For satellite systems that use frequencies at Ka band and above,

all three classes of fade mitigation techniques might be required for high availability links. We will look briefly at each technique.

Power Control

In adaptive power control, the transmitter power is adjusted to compensate for changes in signal attenuation along the path. At its simplest, it is like automatic gain control in a receiver, which adjusts to fluctuations in the received energy so as to hold the receiver output constant. Many satellite links are operated such that the uplink is the critical portion of the connection; that is, the first part of the overall connection that will drop out in a rain fade is the uplink. The overall availability (and performance) of the connection is therefore enhanced if the uplink operates with an increased EIRP in rain. This is referred to as up-link power control (ULPC).

ULPC can operate closed loop, where the signal power is detected at the satellite and a control signal sent back to the earth station to adjust the power, or open loop, where the fade on the downlink signal is used to predict the likely fade level occurring on the uplink. Closed-loop operation is always more accurate but is more expensive to implement; hence most ULPC systems are, at present, open loop.

Open loop ULPC becomes more difficult the further apart the downlink and uplink frequencies are. It becomes even more difficult at Ka band when the downlink (~ 20 GHz) and uplink (~ 30 GHz) frequencies are on either side of the 22-GHz water vapor absorption line. The ratio of 30-GHz attenuation to 20-GHz attenuation is less than 1 for 20-GHz attenuation values of less than 1.0 dB, since cloud attenuation (i.e., essentially water vapor absorption) is higher at 20 GHz than at 30 GHz due to the proximity of the 22-GHz water absorption line to the 20-GHz downlink. Figure 8.27 gives the average 30:20 GHz attenuation ratios, with uplink attenuation as parameter. Note that the long-term 30:20 GHz

attenuation scaling ratio does not become established until the uplink attenuation is above 7 dB. Another major consideration is power flux density variations at the satellite. If many earth stations are operating under rain fade conditions with the same satellite, as could happen in a VSAT network with many hundreds of thousands of earth stations, implementing ULPC can lead to significant received power fluctuations at the satellite, and this has capacity implications. Some of the advanced Ka-band satellites with multiple switched beams can also implement downlink power control, if sufficient bandwidth and power are available.

Signal Processing

The move from very large earth stations (e.g., the Intelsat Standard A) to a multiplicity of small earth stations has been accompanied by a shift in the median traffic stream. It is rare to find a non-video or non-Internet network distribution link via a satellite at a rate of more than 2 Mbit/s. The need to make small traffic streams economic by using VSAT's has led to the introduction of onboard processing (OBP) techniques. This process typically translates the digital carriers arriving at the satellite to baseband for processing and onward transmission back to earth. The process is generically called MCDDD (multi-carrier demodulation, demultiplexing, and decoding). The OBP process is carried out at baseband and allows each individual traffic packet to be switched to the correct output port of the satellite antenna for transmission down to earth following recording and re-multiplexing. By detecting the signal level of each packet on arrival at the OBP, not only can most bit errors be removed but the transmitting earth station can also be alerted if the energy level of the received packet has fallen, so that ULPC can be used at the earth station to correct the signal level (within the power level range of the ULPC system). The use of OBP separates the uplink from the downlink and each part of the link can be treated separately in developing a link budget.

Diversity

Many diversity schemes have been proposed, but few have been implemented as yet due to the cost. If OBP techniques are being used on the satellite, a form of time diversity can be used. In this approach, additional slots in the TDMA frame can be assigned to the rain-affected link so that the same signal can be sent at a slower rate, essentially lowering the bandwidth and raising the C/N. The FEC rate could also be changed in the OBP payload. If the satellite operates in a number of frequency bands (e.g., C band and Ku band), a rain-affected Ku-band link could be switched to C band, which is not attenuated significantly by rain. To be able to do this, spare C-band capacity must be held in reserve on the satellite so that it can be used when required. Similarly, each Ku-band earth station would need to have a dual-band antenna and receiving system so that they could switch between the two bands. The added cost has not justified this approach to date. However, the V-band systems in design at present may find it economic to include a low capacity Ka-band or Ku-band payload to use in those traffic streams that are the highest priority. Of all the diversity schemes, that of site diversity appears to offer the most significant gain in availability.

Site diversity is a technique whereby two, or more, earth stations are located sufficiently far apart to ensure that the paths through the rain that are uncorrelated of individual instantaneous measurements of the uplink and downlink attenuation values. The large range of scaling ratios shows that great care must be taken in developing open-loop algorithms that use only a measure of the amplitude of the downlink frequency.

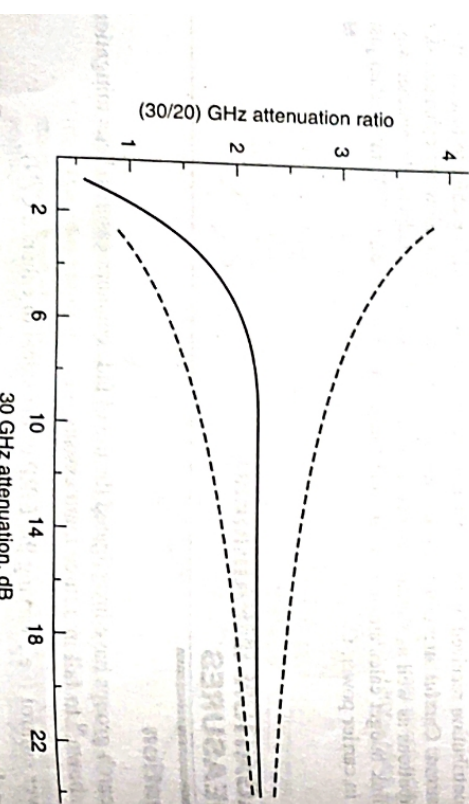


FIGURE 8.27 Instantaneous 30:20 GHz attenuation scaling ratio with 20-GHz attenuation as parameter. The solid curve above is a prediction of the scaling ratio that takes into account both rain attenuation and tropospheric scintillation. The pair of broken curves are the bounds of individual instantaneous measurements of the uplink and downlink attenuation values. The large range of scaling ratios shows that great care must be taken in developing open-loop algorithms that use only a measure of the amplitude of the downlink frequency.

connected together so that any one earth station can be used to support the traffic stream while the other(s) is (are) suffering a rain fade.

If we assume that there are two earth stations, identified by suffixes 1 and 2, which are operated in a site diversity mode, then the *joint attenuation* $A_J(t)$ is defined by

$$A_J(t) = \min[A_1(t), A_2(t)] \text{ dB} \quad (8.41)$$

The average single-site attenuation $A_S(t)$ is the mean of $A_1(t)$ and $A_2(t)$, namely

$$A_S(t) = [A_1(t) + A_2(t)]/2 \text{ dB} \quad (8.42)$$

An ideal system that monitors the received downlink signals at both sites and always selects the stronger of the two experiences an attenuation of $A_J(t)$ and the diversity system would perform better than either site alone. How much better is measured by two statistical quantities, *diversity gain* and *diversity improvement*.

Diversity gain, $G_D(P)$, is the decibel difference between the average single-site attenuation $A_S(P)$ equaled or exceeded $P\%$ of the time and the joint attenuation $A_J(P)$ equaled or exceeded $P\%$ of the time.

$$G_D(P) = A_S(P) - A_J(P) \text{ dB} \quad (8.43)$$

Diversity improvement $I_D(A)$ is the ratio between the percentage of time P_S that the average single-site attenuation A_S exceeds A dB to the percentage of time P_J that the joint attenuation A_J exceeds A dB.

$$I_D(A) = \frac{P_S(A)}{P_J(A)} \quad (8.44)$$

Diversity gain determines system margin, and it is the measure of diversity system performance that we will use here. In addition, diversity gain has been shown to be stable from year to year and, as such, is a reliable statistic to use in system design. Diversity improvement, on the other hand, is extremely variable from year to year. Figure 8.28 illustrates these two concepts.

The first, and still the best, diversity gain model is that due to Hodge³², which has been adapted by the ITU-R in Rec. 618¹⁵. Hodge developed the diversity gain model through an iterative analysis of diversity data available. Intuitively, he assumed site separation was the key element. In this, he has been proved correct. The procedure is abstracted below.

Step 1: Calculate the gain contributed by the spatial separation of the two earth stations from

$$G_d = a(1 - e^{-\kappa d}) \quad (8.45)$$

where d is the separation (km) between the two sites.

$$\begin{aligned} a &= 0.78A - 1.94(1 - e^{-0.11A}) \\ b &= 0.59(1 - e^{-0.1A}) \end{aligned}$$

and A = path attenuation (dB) for a single site.

Step 2: Calculate the frequency-dependent gain from:

$$G_f = e^{-0.0025f} \quad (8.46)$$

where f = frequency (GHz).

Step 3: Calculate the gain term dependent on elevation angle from:

$$G_\theta = 1 + 0.006\theta \quad (8.47)$$

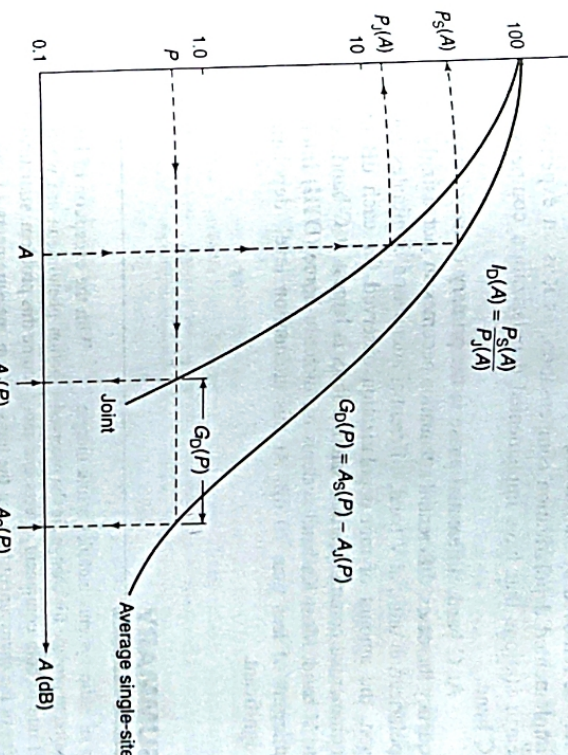


FIGURE 8.28 Illustration of diversity gain and diversity improvement (diversity advantage). At a given percentage of time, P , the diversity gain $G_D(P)$ is the decibel difference between the average single-site attenuation exceeded $A_S(P)$ and the joint attenuation exceeded $A_J(P)$. At a given attenuation, A , the diversity improvement $I_D(A)$ is the ratio of the percentage of time $P_S(A)$ that the single-site attenuation exceeds A to the percentage of time $P_J(A)$ that the joint attenuation exceeds A .

Step 4: Calculate the baseline-dependent term from the expression:

$$G_\psi = 1 + 0.002\psi \quad (8.48)$$

where ψ = angle (degrees) made by the azimuth of the propagation path with respect to the baseline between sites, chosen such that $\psi \leq 90^\circ$.

Step 5: Compute the net diversity gain, G , as the product:

$$G = G_d \times G_f \times G_\theta \times G_\psi \text{ dB} \quad (8.49)$$

The use of a site diversity system is very expensive if traditional approaches are used.

That is, two large earth stations connected together via a very high-speed terrestrial link. It has only been used operationally to date by the gateway stations of the Iridium network. These gateway earth stations operate in Ka band and are single-point failures for the network. As such, the expense of a diversity setup was well justified. Another proposed approach to site diversity has been to use wide area diversity³³, in which a multitude of VSATs are linked via routers to a metropolitan area network.

Depolarization

Depolarization compensation is a technique whereby the feed system of the antenna is adjusted in such a way as to correct for depolarization in the path. Alternatively, the

orthogonal channels may be cross-coupled in the receiver and, provided good samples of the signal in each channel can be obtained, the interfering (i.e., depolarized) signal may be removed by subtracting the correct amount of signal. Few earth stations have implemented depolarization compensation, as it is an expensive undertaking. Those earth stations that have implemented depolarization compensation have done so at C band.

At C band, differential phase is the primary cause of depolarization. As the frequency increases, differential attenuation becomes an increasingly significant cause of polarization until, at V band, differential attenuation dominates completely. For this reason, the amount of rain depolarization observed for each dB of rain attenuation on commercial communications satellite links is largest at C band, reducing monotonically to V band. Most Ka-band systems for direct-to-home (DTH) Internet services have rain margins of less than 10 dB. At this attenuation level, depolarization effects are not significant.

3.8 SUMMARY

The design of radio systems includes a link margin that is intended to provide for changes in the received signal level due to both equipment effects and random changes in the environment between the transmitter and the receiver. The link margin permits the communications system to operate with both the required performance, a measure of the service quality required for a significant fraction of the time, and availability, a measure of the time period when usable service is provided. Developing an adequate link margin is critical to the acceptance of the service. However, each additional dB of link margin that is provided comes with a cost associated with it. A lot of care, therefore, goes into developing an accurate estimate of the likely impairments on any given link that would cause the performance and availability of the service to fall below acceptable levels. A key to this estimate is an understanding of the propagation effects along the path between the satellite and the earth station.

Propagation effects cause two principal phenomena to be observed at the receiving terminal: a change in the wanted signal level, which is referred to as signal attenuation or fading; and a change in the unwanted signal level, which is referred to as depolarization or cross-polarization. Attenuation and depolarization effects are a function of the signal frequency, the atmospheric conditions, and the path geometry. In general, the higher the frequency, the warmer and wetter the weather, and the lower the operating elevation angle of the earth station, the worse the propagation effects are. The only time this is not true is for ionospheric effects, where the effects on commercial satellite systems are only of significance at C band or below.

With the exception of ionospheric effects, propagation phenomena are weather dependent. To overcome this problem, statistical models are used. Long-term measurements of rainfall rate are statistically related to long-term path attenuation measurements when taken over the same period and at the same site. In this case, long-term is at least 1 year so that all of the seasons normally experienced in a given year may be included.

The prediction of rain attenuation has taken two distinct paths: one uses measured data and develops an empirical model to predict the phenomenon on a worldwide basis; the other attempts to model the physics of the process. Statistical models of rain polarization, tropospheric scintillation, gaseous losses, cloud attenuation, low angle fading, and related propagation effects have been developed. Most of these models provide usable predictions for frequencies between 4 and 50 GHz, but care must be taken when predictions for unusual path geometries (e.g., <5°) or severe climates (e.g., tropical regions) are required.

More recently, the impact of individual rain fades—their occurrence statistics, duration of individual events, time between fades of the same level—has become important for developing user perception models for direct-to-home (DTH) services. Counter-measures to rain fades may take many forms—for example, increasing the TDMA frame allocation, changing the power level, changing the modulation index, changing the power level that some ing the frequency—and it is likely that some of them will be included in the Ka-band DTH services planned for the first decade of the twenty-first century.

REFERENCES

- L. J. IRVING, *Propagation Effects Handbook for Satellite Systems Design*, ITT Industries, Advanced Engineering and Sciences, Ashburn, Virginia, Developed for NASA's an update of Reference Publication 1082(04), National Aeronautics and Space Administration, Washington, DC, September 2000.
- J. E. ALLNUTT, *Satellite-to-Ground Radiowave Propagation*, J. E. Allnutt, Wiley Encyclopedia of Electrical and Electronics Engineering, Wiley, ISBN 0 86341 157 6, Peter Peregrinus, 1989 [2nd Ed. in preparation].
- J. E. ALLNUTT, "Refraction and Attenuation in the Transition Region," *Wiley Encyclopedia of Electrical and Electronics Engineering*, John G. Webster, ed., ISBN 0 471 3946 7, Vol. 18, pp. 379–388, 1999.
- A. W. DISSANAYAKE, J. E. ALLNUTT, and F. HADADA, "A Prediction Model that Combines Rain Attenuation and Other Propagation Impairments along Earth-Satellite Paths," *IEEE Transactions on Antennas and Propagation*, Vol. 45, No. 10, October 1997, pp. 1546–1558.
- M. A. B. TERAHA, "Reflector Antennas," *Wiley Encyclopedia of Electrical and Electronics Engineering*, John G. Webster, ed., ISBN 0 471 3946 7, Vol. 18, pp. 360–379, 1999.
- D. C. COX and H. W. ARNOLD, "Comparison of Measured Cross-Polarization Isolation and Discrimination for Rain and Ice on a 19 GHz Space-Earth Path," *Radio Science*, 19, 617–628, March–April 1984.
- P. N. KUMAR, "Depolarization of 19 GHz Signals," *Comsat Technical Review*, 12, 271–293, Fall 1982.
- ACTS experimental results, presented in a series of proceedings, e.g., *Proceedings of the Twenty-third NASA Propagation Experimenters Meeting (NAPEX XXIII)* and *the Advanced Communications Technology Satellite (ACTS) Propagation Studies Workshop*, Nasar Golshan and Christian Ho, eds., Falls Church, Virginia, June 2–4, 1999. For updated information, see the NASA web site.
- OLYMPUS Propagation Experiment (OPEX), Second Workshop of the Olympus Propagation Experimenters, WPP-083, Volumes 1 (Attenuation Measurement and Prediction), 2 (Depolarization), 3 (Radiometry and Meteorological Measurements), 4 (Radar), and 5 (Data Processing), Nordanwijk, The Netherlands, 8–10 November 1994.
- P. A. WATSON, and M. ARABI, "Cross-Polarization Isolation and Discrimination," *Electronics Letters*, 9, November 1973, 516–519.
- Rec. ITU-R P.676-3, *Attenuation by Atmospheric Gases*, 1997.
- A. W. DISSANAYAKE, J. E. ALLNUTT, and F. HADADA, "A Prediction Model that Combines Rain Attenuation and Other Propagation Impairments along Earth-Satellite Paths," *IEEE Transactions on Antennas and Propagation*, Vol. 45, No. 10, pp. 1546–1558, October 1997.
- E. SALONEN, and S. UPPALA, "New Prediction Method of Cloud Attenuation," *Electronics Letters*, Vol. 27, No. 12, pp. 1106–1108, 1991.
- A. W. DISSANAYAKE, J. E. ALLNUTT, and F. HADADA, "Cloud Attenuation Modeling for SHF and EHF Applications," Invited paper, Special Issue of International Journal of Satellite Communications, revised and accepted, January 2000.
- Rec. ITU-R P.618-6, *Propagation Data and Prediction Methods Required for the Design of Earth-Space Telecommunications Systems*, 1999.
- T. PEART, and D. J. BROWNING, "Co-polar Attenuation and Radiometer Measurements at 30 GHz for a Slant Path to Central England," *Proceedings ATS-6 Meeting (ESA SP-131)*, ESTEC, Noordwijk, The Netherlands, 15–20 October 1977.
- E. C. JOHNSTON, D. L. BRYANT, D. MARTIN, and J. E. ALLNUTT, "Results of Low Elevation Angle 11 GHz Satellite Beacon Measurements at Goonhilly," *IEE Conference Publication No. 333*, ICAP 91, pp. 366–369, April 1991.
- K. MUUSLUU, and T. UICH, "A New Method to Determine the Solar Cycle Length," *Geophysical Research Letters*, 25, 1837–1840, 1998.
- Rec. ITU-R PN 837-1, *Characteristics of Precipitation for Propagation Modelling*, 1994.
- The general web site for the ITU is <http://www.itu.int/bwgsg3/>. For ITU model software see <http://www.itu.int/bwgsg3/databank/tropospheric.html>
- Report 564 of the *Recommendations and Reports of the CCIR, Volume V, Propagation in Non-Ionized Media*, International Telecommunications Union (ITU), Geneva, Switzerland, 1982.
- Rec. ITU-R P.837-2, *Characteristics of Precipitation for Relation in the Calculation of Rain Attenuation*, "IEEE Transactions on Antennas and Propagation AP-26, 318–329, March 1978.
- M. P. M. HALL, *Effects of the Troposphere on Radio Communication*, Peter Peregrinus, Ltd., Stevenage, UK, 1979.
- R. L. OLSEN, D. V. ROETERS, and D. B. HOOD, "The ACTS Rain Attenuation Model," *IEEE Transactions on Antennas and Propagation*, Vol. 41, No. 1, pp. 1029–1078, September 1993.
- T. OUCHI, "Electromagnetic Wave Propagation and Scattering in Rain and Other Hydrometeors," *Proceedings of the IEEE*, 71, 1029–1078, September 1983.
- Rec. ITU-R P.838, *Specific Attenuation Model for Rain for Use in Prediction Methods*, 1992.
- C. W. BOSTIAN, and D. V. ROETERS, "System Implications of 14/11 GHz Path Depolarization. Part II: Reducing the Impairments," *International Journal of Satellite Communications*, 4, 13–17, 1986.
- F. BARABASCH, A. PARABONI, and C. RIVA, *Private communication*, December 1999.
- L. CASTANET, J. LEMORTON, and M. BOUSQUET, "Fade Mitigation Techniques for New SatCom Services at Ku-Band and Above: A Review," *COST 255 First International Workshop on Radiowave Propagation Modelling*, No. 12, pp. 1106–1108, 1991.